

ORIGINAL ARTICLE

Population Pharmacokinetics and Pharmacodynamics of Lampalizumab Administered Intravitreally to Patients With Geographic Atrophy

KN Le^{1*}, L Gibiansky², M van Lookeren Campagne¹, J Good¹, T Davançaze¹, KM Loyet¹, A Morimoto¹, EC Strauss¹ and JY Jin¹

Intravitreally administered lampalizumab is an investigational complement inhibitor directed against complement factor D (CFD) for the treatment of geographic atrophy (GA) secondary to age-related macular degeneration. We sought to develop an integrated ocular and systemic pharmacokinetic/pharmacodynamic model for lampalizumab in patients with GA using the data from the clinical phase I and II studies. The kinetics of lampalizumab and CFD disposition were well described by the combined ocular/serum target-mediated drug disposition model using a quasi-steady-state approximation. This model takes into account the drug, target, and drug–target complex clearance, their transfer rates between ocular and serum compartments, and turnover kinetics of CFD. The constructed model provided a prediction of target occupancy in ocular tissues and supported that the two dosing regimens (10 mg q4w and 10 mg q6w) selected for the phase III studies are expected to be efficacious and able to achieve near-complete target engagement in the vitreous humor.

CPT Pharmacometrics Syst. Pharmacol. (2015) 4, 595–604; doi:10.1002/psp4.12031; published online on 8 October 2015.

Study Highlights

WHAT IS THE CURRENT KNOWLEDGE ON THE TOPIC? A quantitative understanding of the lampalizumab pharmacokinetics is crucial in interpreting the results of clinical studies of lampalizumab and determining the dosing schedule for phase III trials. • WHAT QUESTION DID THIS STUDY ADDRESS? A population PK/PD model was developed to describe ocular and serum concentration–time profile and evaluate target occupancy following intravitreal lampalizumab to increase our understanding of lampalizumab PK/PD characteristics in patients with GA. • WHAT THIS STUDY ADDS TO OUR KNOWLEDGE This study describes the PK/PD characteristics of lampalizumab, which is critical to help guide the rational design of phase III trials and to interpret the safety and efficacy data in patients with GA. • HOW THIS MIGHT CHANGE CLINICAL PHARMACOLOGY AND THERAPEUTICS These analyses represent the first TMDD model to guide rational study design and regimen selection in ophthalmology drug development. The combined ocular/serum TMDD model using quasi-steady-state approximation that takes into account factors of the specific molecule may provide a useful framework for describing other biologics for intravitreal administration.

Age-related macular degeneration (AMD) is an irreversible and progressive disease that develops from early and intermediate stages into the two advanced forms known as geographic atrophy (GA) and neovascular AMD. GA is a significant unmet need, affecting more than 5 million people worldwide, with devastating effects on patients' visual function and quality of life.^{1,2} GA is characterized by extensive loss of the choriocapillaris and the overlying retinal pigment epithelium (RPE), and accounts for 26% of legal blindness in the United Kingdom.^{3–6} Currently, there are no licensed therapies to prevent the progression of GA and the associated decrease in visual function.⁷

Lampalizumab is a first-in-class investigational drug currently being developed for the treatment of GA secondary to AMD. Lampalizumab is the antibody binding fragment (Fab) of a humanized monoclonal antibody (mAb) directed against complement factor D (CFD), a rate-limiting enzyme involved in the activation of the alternative complement pathway and its amplification via the feedback loop, which has been implicated in GA.^{8,9} Lampalizumab, previously

referred to as FCFD4514S, was investigated in the completed phase Ia single ascending-dose clinical study¹⁰ (CFD4711g; NCT00973011) and in the MAHALO phase Ib/II clinical trial (CFD4870g; NCT01229215, unpublished data). Lampalizumab binds with high affinity to both cynomolgus monkey ($K_D = 11.7$ pM) and human ($K_D = 19.7$ pM) CFD.¹¹ The systemic pharmacokinetics (PK) of lampalizumab in patients with GA were characterized in the phase Ia study,¹⁰ with a systemic elimination half-life ($t_{1/2}$) following intravitreal administration of 5.9 days.

The ocular and systemic PK following intravitreal (ITV) administration of large molecules, including Fabs and mAbs, have been studied extensively.^{12–18} In clinical studies, ranibizumab, an anti-vascular endothelial growth factor (VEGF)-A Fab, was observed to clear from the eye with a half-life of 9 days and, upon reaching the systemic circulation, clear more quickly, with a half-life of 2 hours.¹⁹ In preclinical models, ranibizumab was shown to distribute rapidly to the retina¹⁶ and penetrate all retinal layers.¹⁵ The ocular and systemic PK of a full-length antibody, bevacizumab, and a receptor

¹Genentech, South San Francisco, California, USA; ²Quantpharm, North Potomac, Maryland, USA. *Correspondence: KN Le (knle@alum.mit.edu)
Received 29 May 2015; accepted 11 August 2015; published online on 8 October 2015. doi:10.1002/psp4.12031

fusion protein, aflibercept, have also been widely investigated. The ocular half-life of bevacizumab, a full-length mAb that binds all isoforms of VEGF-A, was shown to be 9.8 days.¹⁷ Once absorbed into the systemic circulation, ranibizumab clears quickly as a result of its relatively smaller size, whereas bevacizumab and aflibercept have greater systemic exposure that results in a marked reduction in free VEGF in the plasma.⁵ Prior studies of anti-VEGF agents have contributed greatly to our understanding of how large molecules distribute in and eliminate from the ocular compartments and systemic circulation upon ITV administration. Yet limited studies have integrated ocular and systemic data on drugs and their binding target to offer knowledge of target engagement, which is crucial to the selection of appropriate dosing regimens. The current analyses aimed to establish a semimechanistic model that describes the systemic and ocular disposition of lampalizumab and CFD following ITV administration of single and multiple lampalizumab doses in patients with GA. We built a target-mediated drug disposition (TMDD) model that incorporated the binding quasi-steady-state assumption, and turnover rates of CFD, lampalizumab, and lampalizumab–CFD complex. In addition, model-based simulations of clinically relevant dosing regimens were performed to illustrate concentration–time courses of ocular and serum drug concentrations and predict ocular CFD occupancy that supported the dosing regimens in the phase III trials. These analyses also represented the first TMDD model to guide rational study design in ophthalmology drug development.

METHODS

Study design

For population PK/PD analysis, the data from two studies shown in **Table 1** were integrated. Both studies received approval from the Institutional Review Board at each study site and all participants provided written informed consent. In Study CFD4711g, a total of 18 patients (three per dose level) received a single ITV administration of lampalizumab at dose levels of 0.1, 0.5, 1, 2, 5, and 10 mg in the study eye. Lampalizumab serum concentration data were obtained at screening, and at 1, 7, 14, and 30 days post-dose. Study CFD4870g was a multidose study that included a run-in safety assessment phase and a randomized phase. In the safety run-in phase, patients ($n = 14$) received a minimum of three monthly doses of 10 mg ITV lampalizumab. Serum lampalizumab concentration data were obtained at screening, and predose (trough) at months 1, 2, and 3. These patients then proceeded with the same dosing frequency for the remainder of the 18-month treatment period. In the phase II component of Study CFD4870g, patients ($n = 129$) were randomized to one of the two active arms (10 mg every month or 10 mg every other month) or to the corresponding sham injection arms. In the randomized phase II study, the serum lampalizumab concentration was collected at screening, at 1, 2, 3, 6, 9, 12, 15, and 18 months predose (trough), and at 7 days postdose. In addition, aqueous humor concentrations of lampalizumab and total CFD were measured at screening, 6 months predose, and 12 months predose (data available from 12 patients).

PK/PD model structure

Ocular and serum concentration analysis using a TMDD model. Lampalizumab ocular (aqueous humor) and serum concentrations in patients with GA were analyzed using a TMDD model that incorporated the binding quasi-steady-state assumption, and *in vivo* turnover rates of CFD, lampalizumab, and lampalizumab–CFD complex. The IMPMAP method of NONMEM software was used to estimate model parameters, as it was shown to be fast and efficient for problems with TMDD.^{20,21}

A quasi-steady-state approximation²² of the target-mediated drug disposition model described the total (unbound and bound to CFD) vitreous humor lampalizumab concentrations and total (unbound and bound to lampalizumab) vitreous humor CFD concentrations. Both lampalizumab and lampalizumab–CFD complex were assumed to egress to the systemic circulation where total (unbound and bound to CFD) lampalizumab clearance was described by a linear elimination process. Equations that describe the final model are provided below:

$$\frac{dA_{VITR}}{dt} = -k_{out} \cdot C_{unbound} \cdot V_{VITR} - k_{outC} \frac{R_{VITR} \cdot C_{unbound} \cdot V_{VITR}}{K_{ss} + C_{unbound}} \quad (1)$$

$$\frac{dR_{VITR}}{dt} = k_{inT} - k_{outT} \cdot R_{VITR} - (k_{outC} - k_{outT}) \cdot \frac{R_{VITR} \cdot C_{unbound}}{K_{ss} + C_{unbound}} \quad (2)$$

$$\frac{dA_{SER}}{dt} = k_{out} \cdot C_{unbound} \cdot V_{VITR} + k_{outC} \frac{R_{VITR} \cdot C_{unbound} \cdot V_{VITR}}{K_{ss} + C_{unbound}} - k \cdot A_{SER} \quad (3)$$

$$C_{unbound} = \frac{1}{2} [(C_{VITR} - R_{VITR} - K_{ss}) + \sqrt{(C_{VITR} - R_{VITR} - K_{ss})^2 + 4 \cdot K_{ss} \cdot C_{VITR}}] \quad (4)$$

$$C_{AQ_tot} = \frac{C_{VITR}}{\lambda_{AQ}} \quad (5)$$

$$R_{AQ} = \frac{R_{VITR}}{\lambda_{TAQ}} \quad (6)$$

$$\lambda_{TAQ} = \lambda_{AQ} \lambda_A \quad (7)$$

Here Eqs. 1 and 2 describe the kinetics of lampalizumab amount (A_{VITR}) and total CFD amount in vitreous humor (R_{VITR}), respectively. Eq. 3 describes the lampalizumab amount in serum (A_{SER}). Eq. 4 describes the quasi-steady-state approximation for the relationship between unbound lampalizumab concentration ($C_{unbound}$), total lampalizumab concentration (C_{VITR}), and total CFD concentration (R_{VITR}) in vitreous humor. Eq. 5 describes the relationship between aqueous humor (C_{AQ_tot}), vitreous humor (C_{VITR}) total lampalizumab concentration, and the aqueous-vitreous humor lampalizumab partition coefficient (λ_{AQ}). Eq. 6 describes the relationship between total CFD level in aqueous humor (R_{AQ}), vitreous humor (R_{VITR}), and aqueous-vitreous humor partition coefficient of total CFD (λ_{TAQ}). Eq. 7 describes the relationship between the partition coefficient of lampalizumab and CFD to the correction ratio that was estimated by

Table 1 Model parameter estimates using the ocular-serum TMDD model

Parameter	Symbol (unit)	Estimate	RSE (%)	95% CI		Shrinkage (%)
				Lower	Upper	
<u>Ocular parameters</u>						
Ocular elimination rate constant of drug ^a	k_{out} (1/day)	0.117	1.25	0.111	0.123	
Ocular elimination rate constant of complex	k_{outC} (1/day)	0.135	1.54	0.127	0.144	
Ocular influx/synthesis rate constant of target	k_{inT} ($\mu\text{g}/\text{mL}/\text{day}$)	0.364	0.635	0.360	0.369	
Correction factor for drug:target molar ratio and assay differences ^c	λ_A	2.23	27.7	1.440	3.46	
Vitreous volume of distribution	V_{VITR} (mL)	3.09	3.24	2.88	3.23	
Ocular degradation/elimination rate constant of drug target	k_{outT} (1/day)	0.27	0.935	0.236	0.276	
Vitreous-aqueous partition coefficient of drug	λ_{AQ}	13.0	0.586	12.7	13.4	
<u>Systemic parameters</u>						
Systemic volume of distribution	V_C (mL)	2410	0.0658	2390	2440	
Systemic elimination rate constant of drug ^a	k (1/day)	1.89	6.53	1.74	2.05	
Quasi-steady rate constant ^d	K_{SS} ($\mu\text{g}/\text{mL}$)	0.96×10^{-3} (fixed)				
<u>Covariates</u>						
Power for age effect on k_{out}	$\Theta_{age-kout}$	-0.770	45.5	-1.45	-0.0831	
Power for age effect on k	Θ_{age-k}	-1.63	23.5	-2.38	-0.877	
Multiplier for sex effect on k	Θ_{sex-k}	0.739	21.1	0.652	0.837	
<u>Variability</u>						
Intersubject variability for ocular clearance	ω_{kout}^2	27.3%	19.1 ^b	21.6%	32.0%	6.3
Intersubject variability for correction factor	$\omega_{\lambda_A}^2$	59.1%	38.0 ^b	29.8%	78.0%	0.8
Intersubject variability for systemic clearance	ω_k^2	27.5%	23.8 ^b	20.1%	33.3%	20.7
Residual error for aqueous measurements	$\sigma_{prop, AQ}^2$	25.8%	28.3 ^b	17.2%	32.2%	
Residual error for serum measurement	$\sigma_{prop, SER}^2$	32.9%	10.1 ^b	29.5%	36.1%	

CI, confidence interval; RSE, relative standard error.

^aFor a typical 80-year-old male patient.^bRSE for variances.^cRatio of the molecular weights of the drug and the target is equal to 2 (within 95% CI of the estimated value). Minor difference with the estimated value could be due to assay differences or differences in volumes of distributions of the drug and the target.^dFixed to 20 pM, approximately equal to *in vitro* KD value (19.7 pM), as the estimated elimination rate of the drug-target complex (k_{outC}) is much smaller than dissociation rate of the drug-target complex.^{8,11}

the model (**Table 1**). In our model, the free CFD and lampalizumab-CFD complex were assumed to partition across the aqueous humor, vitreous humor, and retina in a similar fashion.

V_{VITR} and V_C are the vitreous humor and serum volumes, respectively; R_{AQ} is the total CFD concentration in aqueous humor; k_{out} and k_{outC} denote the elimination rate constants of the unbound lampalizumab and lampalizumab-CFD complex, respectively. The clearance of the complex in the aqueous humor was not explicitly modeled and was implicitly assumed to follow similar clearance kinetics to that in the vitreous humor and was accounted for by the constant partition coefficient of the total lampalizumab (λ_{AQ}) and total CFD (λ_{TAQ}) between the aqueous and vitreous humors. λ_{TAQ} was calculated using Eq. 7, where λ_A is a correction factor accounting for the differences in molecular weight of drug and target. k_{inT} and k_{outT} are zero-order production and first-order degradation rate constants of CFD in vitreous humor, respectively; k is the first-order clearance rate constant of lampalizumab in serum; K_{SS} is the quasi-steady-state constant of lampalizumab binding to CFD.

Two levels of random effects were included in the model: intersubject variability and within-subject variability. Intersubject variability was added to recognize differences between

individuals and was described by log-normal parameter distributions with zero means. The within-subject variability (residual error model) for the observations is described by a proportional error model, and the proportional residual errors are assumed to be independent and normally distributed with zero means. Initially, intersubject variability was estimated on all parameters as required for the efficient implementation of the IMPMAP method.^{20,21} After the model was developed, variance parameters were tested one by one by fixing the coefficient of variation (CV) to 1%, applying the backward elimination procedure with $\alpha = 0.01$ significance level. Only three random effect parameters (k_{out} , k , and λ_a) were significantly different from 1%.

Covariate analysis

After the base model was developed, effects of age, sex, and antiatherapeutic antibodies (ATA) status on k_{out} and k were added to the model. Effects of age and sex were of clinical interest. ATA status was selected because it has been shown to have an effect on the pharmacokinetics for some biologics.^{23–25} As the number of subjects in the dataset was small, the goal was to capture the most important effects rather than perform a comprehensive evaluation of the covariate model. Therefore, covariate effects were

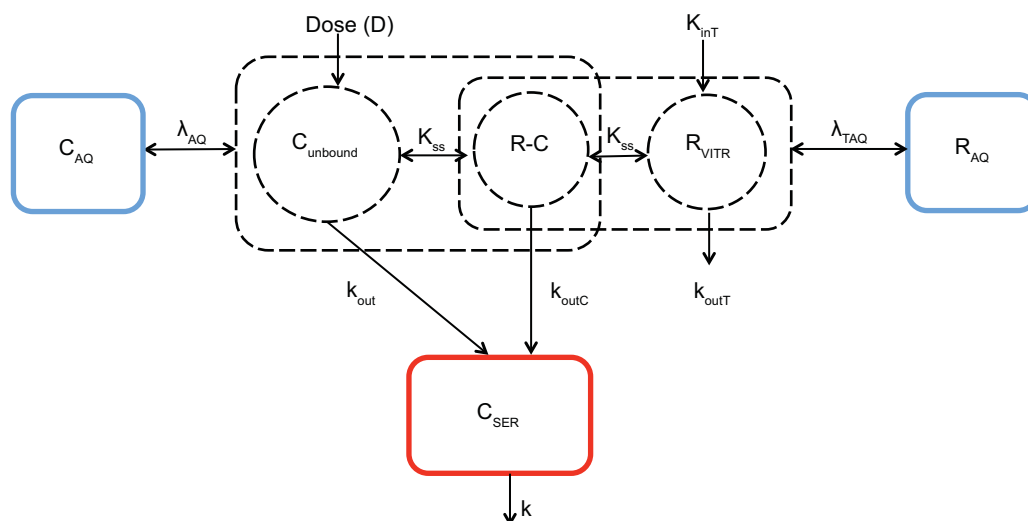


Figure 1 Target-mediated drug disposition (TMDD) model schematic describing lamalizumab ocular and systemic pharmacokinetics. C_{unbound} , R_{VITR} , and $R\text{-}C$ compartments represent the free drug, free target, and drug–target complexes in the vitreous humor, respectively. C_{AQ} and R_{AQ} represent total drug and total target in the aqueous humor, respectively. C_{SER} represents total drug in serum. k_{out} and k represent ocular and systemic elimination constants of drug. k_{outT} and k_{outC} represent ocular elimination rate of target and complex, respectively. k_{int} represents the combined rate of synthesis and/or influx of target into the eye. K_{ss} represents the quasi-steady-state equilibrium constant. λ_{AQ} and λ_{TAQ} represent vitreous-aqueous humor partition coefficients of drug and target, respectively. Square boxes represent total (free and bound) analytes. Circle boxes represent analytes in either free or complex form. Dotted boxes represent hypothetical compartments, and solid boxes represent those with measured data.

tested only on ocular (k_{out}) and systemic elimination rate constants (k), which are the main parameters that govern the ocular and systemic pharmacokinetics, respectively.

Backward elimination procedure with $\alpha = 0.01$ significance level was applied to arrive at a parsimonious final model.

RESULTS

Serum pharmacokinetics

The database for systemic population lamalizumab PK analysis contained data from a total of 117 patients with GA in both phase Ia and Ib/II studies (**Supplemental Table 1**). A total of 697 quantifiable concentrations, which were greater than the lower limit of quantitation (LLOQ = 350 pg/mL), were used for model building.

A one-compartment population PK model was shown to be adequate to describe the lamalizumab PK in the systemic circulation using only the serum dataset (**Supplemental Figure 1**) or the combined ocular/serum dataset (**Figure 1**). The diagnostic plots indicated a good fit of the model to the data, at both the individual and population levels (**Figure 2** and **Supplemental Figure 2**). Systemic half-life was estimated to be 9 hours ($k = 1.89 \text{ day}^{-1}$, **Table 1**) when using the combined ocular/serum model, and was in agreement with the population serum PK model ($t_{1/2} = 7.4$ hours, $k = 2.23 \text{ day}^{-1}$, **Supplemental Table 2**). Furthermore, both population and individual predictions from the two models were well correlated (**Supplemental Figure 2C**), suggesting that the incorporation of ocular PK had no impact on serum PK characterization. The parameter estimates of the model fit to only the serum dataset are presented in **Supplemental Table 2**.

All parameters were estimated precisely with relative standard error (RSE) values of 2.7–12.9%.

Ocular pharmacokinetics

The database for the combined ocular/systemic population lamalizumab PK/pharmacodynamic (PD) analysis contained data from the systemic concentrations dataset ($n = 697$ concentrations) and ocular dataset, which included a total of 24 quantifiable aqueous humor lamalizumab (LLOQ = 30 ng/mL) and 62 quantifiable aqueous humor total CFD (LLOQ = 5 ng/mL) concentrations from a total of 21 patients (**Supplemental Table 1**).

A TMDD model with a quasi-steady-state approximation of ocular binding kinetics was shown to be adequate to describe the total (unbound and bound to CFD) aqueous humor lamalizumab concentrations and total (unbound and bound to lamalizumab) aqueous humor CFD concentrations (**Figure 1**). The final model with constant vitreous-to-aqueous humor partition coefficients for lamalizumab ($\lambda_{\text{AQ}} = 13.0$) and CFD ($\lambda_{\text{TAQ}} = \lambda_{\text{AQ}} \times \lambda_{\text{A}} = 29.0$, where $\lambda_{\text{A}} (=2.23)$ was a correction factor for molecular weight described in **Table 1**) can adequately describe the relationship between the vitreous and the aqueous humor concentrations of lamalizumab and CFD. These results showed that the observed aqueous humor concentrations were linearly proportional to the corresponding model-predicted vitreous humor concentrations, and suggested that lamalizumab reached equilibrium relatively quickly across aqueous and vitreous humors.

The parameter estimates of the integrated ocular/systemic PK model are presented in **Table 1**. The model diagnostic plots indicated that model-predicted concentrations of lamalizumab in serum and aqueous humor as well as total CFD in aqueous humor were in good agreement with the observed

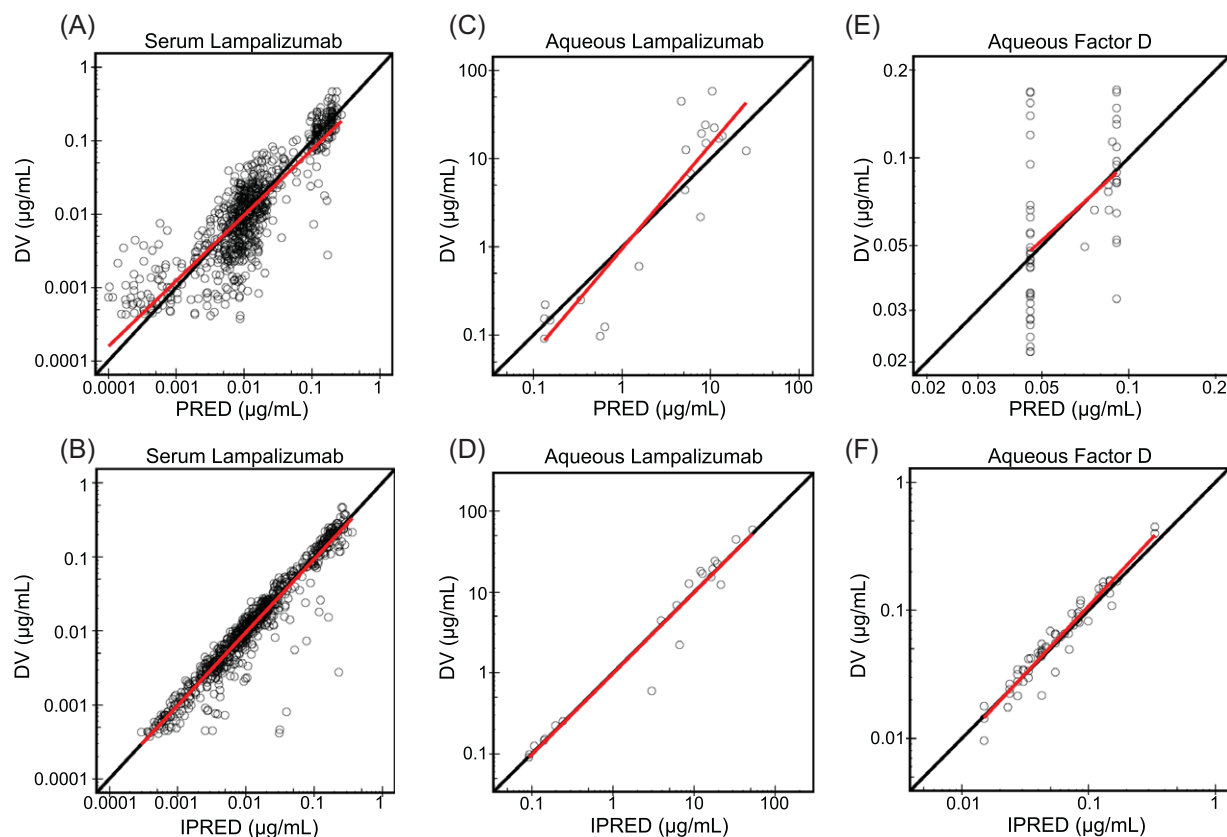


Figure 2 Comparison of observed data to population and individual model predictions for serum lampalizumab (a,b), aqueous humor lampalizumab (c,d), and aqueous humor total complement factor D (e,f). DV denotes dependent variable or observed data. PRED denotes model-predicted population values. IPRED denotes model-predicted individual values. Solid red lines represent linear regression lines. Solid black lines represent lines of unity.

data (Figure 2). Also in agreement with the serum population PK model, ocular-to-systemic absorption half-life was estimated to be 5.9 days ($k_{out} = 0.117 \text{ day}^{-1}$).

Visual predictive checks (Figure 3) confirmed good predictive power of the final TMDD model in predicting serum and aqueous humor lampalizumab as well as aqueous humor total CFD concentrations simultaneously. The 90% prediction interval and median were obtained by simulating 1,000 datasets using the final integrated PK/PD model. The model adequately described the observed serum concentrations for both monthly and every-other-month regimens. Despite the small number in aqueous humor sample size, the aqueous humor lampalizumab and total CFD were reasonably predicted up to day 60 postdose.

Simulation of vitreous humor and serum steady-state lampalizumab concentrations

Model-based simulations were conducted to examine steady-state vitreous humor and serum exposures of lampalizumab following a similar 10-mg ITV dose administration with alterations in schedule, including every 4 weeks (q4wk), every 6 weeks (q6wk), and an every 8 weeks (q8wk) regimen (Figure 4). Lampalizumab reached maximum concentrations (C_{max}) in the serum within ~ 1 day following ITV administration. As no accumulation in vitreous humor and serum was observed for

all three regimens, steady-state lampalizumab exposure in vitreous humor and serum was similar to that following the first dose. At steady-state, lampalizumab vitreous humor exposure was greater than 11,000-fold higher than serum exposure based on serum and vitreous humor C_{max} , minimum concentrations (C_{min}), or cumulative area under the concentration–time curve ($AUC_{0-72\text{wk}}$) (Supplemental Table 3).

Additionally, with all three dosing schedules, the 5th percentile of vitreous humor C_{min} values for 10 mg per eye were above the median inhibitory concentration (IC₅₀) ($\sim 0.2 \mu\text{g/mL}$ or 4 nM) of alternative complement inhibition (Figure 4a and Supplemental Table 3) based on a serum hemolytic cell-based assay,¹¹ while the 95th percentile of serum C_{max} values for 10 mg per eye were below $2 \mu\text{g/mL}$ or 42 nM (Figure 4b and Supplemental Table 3), the minimum level needed to inhibit alternative complement pathway in the serum.^{10,11} Our simulations showed that intravitreally administered lampalizumab results in high local ocular drug concentrations while minimizing systemic drug concentrations and potential systemic adverse events.

Covariate analysis

Covariate analysis was performed to identify major factors predictive of variability in lampalizumab ocular and

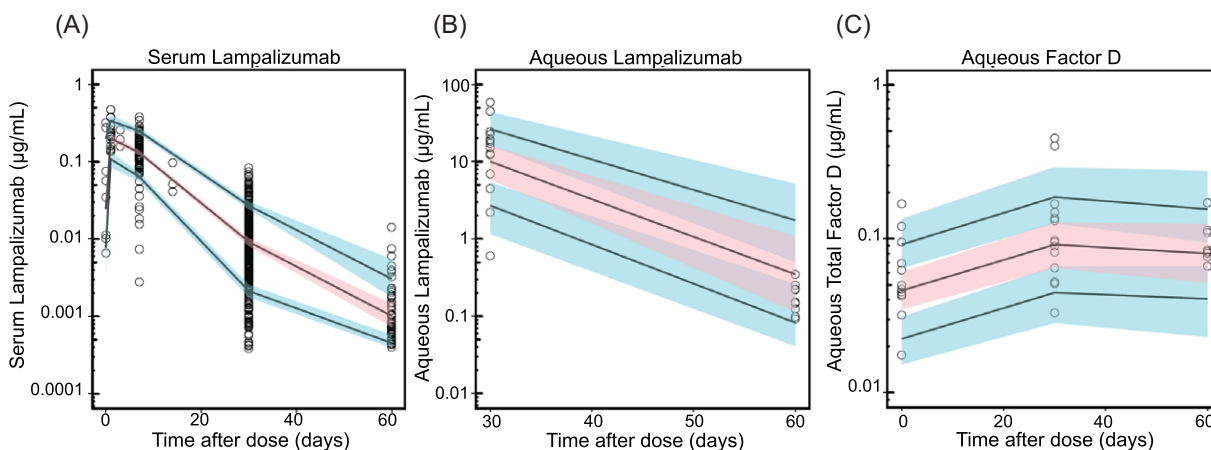


Figure 3 Visual predictive checks (VPCs) of final model fitted to the combined ocular-serum dataset demonstrating good predictive power of concentration-time profiles of serum lampalizumab (a), aqueous humor lampalizumab (b), and aqueous humor total complement factor D (c). Black open circles represent observed data. Solid black lines represent 10th, 50th, and 90th percentiles of the simulation-based concentrations. Red regions represent 10th–90th confidence intervals of the 50th model-predicted concentrations. Blue regions represent the 10th–90th confidence intervals of the 10th and 90th model-predicted concentrations.

systemic PK. Sex, age, and ATA status were tested as covariates on k_{out} and k . ATA status was not a statistically significant covariate for either k_{out} or k . Age was found to be a statistically significant covariate explaining intersubject variability for both k_{out} (3.6%) and k (7.6%), whereas sex was a statistically significant covariate explaining intersubject variability for k_{out} (11.5%). Older patients and females appeared to have a slower systemic elimination constant (k) or longer systemic half-life (**Supplemental Figure 3A**). Older patients also tended to have a slower ocular elimination constant (k_{out}) and longer ocular half-life (**Supplemental Figure 3B**). To examine the impact of age and sex on the clinically relevant ocular and systemic exposures, the magnitude of their covariate effect on ocular C_{min} , cumulative AUC, serum C_{max} , and cumulative AUC was examined (**Figure 5**). Despite the statistically significant impact of age and sex on k and age on k_{out} , the magnitude of the covariate effects was relatively small compared to the intersubject variability and was not expected to be clinically relevant.

Simulation of ocular target suppression

Simulations based on the integrated ocular/systemic TMDD PK model were performed to predict the ratio of free target (FTR) following lampalizumab administration to that at baseline (FTR = free target/total target at baseline) in the vitreous humor to aid in dosing selection for future clinical studies. Single-dose simulations were presented because the ocular concentrations reached steady-state following the first dose, as evidenced by the absence of accumulation with repeat dosing (**Figure 4a**). The simulations showed that the free target (CFD) level was substantially suppressed compared to baseline level at up to day 60 postdose (**Figure 6**), which indicated approximately complete target inhibition of the alternative complement pathway in the vitreous humor with all three schedules of the 10-mg dose.

DISCUSSION

In this analysis, we developed a population TMDD model based on data from the phase I and II studies to describe the ocular and systemic PK and PD of lampalizumab. The serum/aqueous humor lampalizumab and aqueous humor total CFD concentration–time data in patients with GA who received intravitreal lampalizumab was accurately described by an integrated ocular/serum PK model.

Using standard goodness-of-fit criteria and visual predictive checks, the best ocular PK model that described the lampalizumab PK/PD data and had good predictive power is one that included the target-mediated drug disposition in the eye with a quasi-steady-state assumption, first-order ocular clearance of unbound lampalizumab and lampalizumab–CFD complex, and quick equilibrium between vitreous and aqueous humor compartments (**Figure 1**). Systemic PK of total (free and bound) lampalizumab was well described by a linear first-order clearance (**Figure 1** and **Supplemental Figure 1**).

The ocular half-life of lampalizumab was estimated to be ~6 days, which is consistent with the noncompartmental analysis of lampalizumab PK in the phase Ia study.¹⁰ This was also similar to the ocular half-life of ranibizumab of 7 to 9 days,^{18,19} an intravitreally administered Fab. The lampalizumab PK following ITV administration in humans was shown to exhibit flip-flop PK, which is consistent with the lampalizumab PK in monkeys¹¹ and ranibizumab PK in both monkeys²⁶ and humans.¹⁹ This is a phenomenon in which the rate of drug cleared from the systemic circulation is much faster than the rate of drug egressing out of the vitreous humor. This occurs for the lampalizumab Fab drug platform (and all Fab fragments) as a result of lacking the Fc region, which is the portion of antibodies responsible for recirculation into the systemic circulation and prolonging the systemic half-life. Notably, faster systemic clearance compared with ocular clearance of ranibizumab was likewise associated with the lack of an Fc region. In fact, ranibizumab was

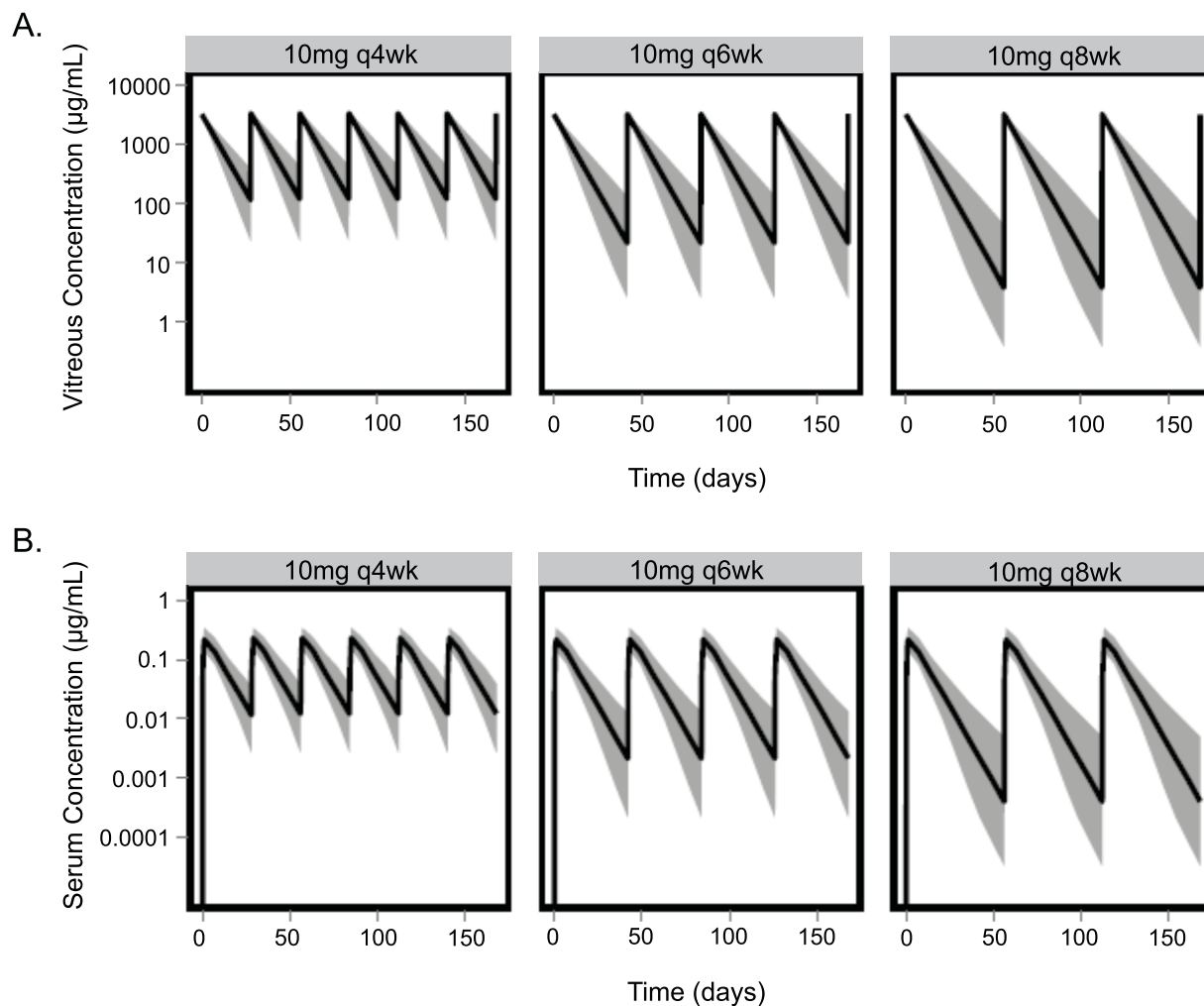


Figure 4 Population prediction of vitreous humor (a) and serum (b) concentration-time profiles with q4wk, q6wk, and q8wk of lampalizumab at dose level of 10 mg per eye. Black solid lines represent 50th percentile of the population, and shaded regions represent 5th–95th prediction intervals.

shown to have a rapid systemic clearance upon egressing into the systemic circulation following ITV administration and substantially lower systemic exposure compared with bevacizumab and aflibercept, which both contain an Fc region.¹² Importantly, the flip-flop PK phenomenon enabled the use of systemic half-life following ITV administration as a surrogate for ocular half-life for intravitreally administered drugs when ocular sampling for drug concentration measurements may not be possible or convenient.

Due to the limited sample size and sparse sampling of the ocular PK/PD samples, one concern was whether the individual ocular lampalizumab prediction could be accurately estimated. To evaluate the accuracy of the individual ocular PK predictions using the combined ocular/systemic TMDD model, we built an additional systemic PK model, which was shown to meet model evaluation criteria (**Supplemental Table 2** and **Supplemental Figure 2**). The parameters in the systemic PK model were estimated with good precision and low shrinkage (**Supplemental Table 2**). Additionally, the systemic PK model correlated well with the

individual predictions from the ocular/systemic TMDD model. Therefore, the ocular/systemic TMDD model was suitable to describe both ocular lampalizumab/total CFD and systemic lampalizumab for the individual patients in the study. This model could be used to predict ocular lampalizumab exposure and total CFD upon ITV administration of lampalizumab in GA patient populations as well as in the individual patients in these studies.

This model-based analysis also revealed that the combined CFD ocular influx and ocular production rate were substantially lower than the systemic CFD production rate. Current literature suggests that CFD synthesis in the systemic circulation is fast, with an estimated rate of 1.33 mg/kg/day in humans.²⁷ Our model did not distinguish whether the local ocular CFD influx comes from the systemic circulation or *de novo* synthesis. However, the composite influx rate (k_{inT}) of CFD into the ocular compartment estimated from the study model was 0.32 µg/mL/day (**Table 1**) or 0.91 µg/day (with $V_{VITR} = 2.85$ mL), which amounts to less than 1% of systemic production

Steady State Exposure Following 10 mg/Eye q4wk Dosing

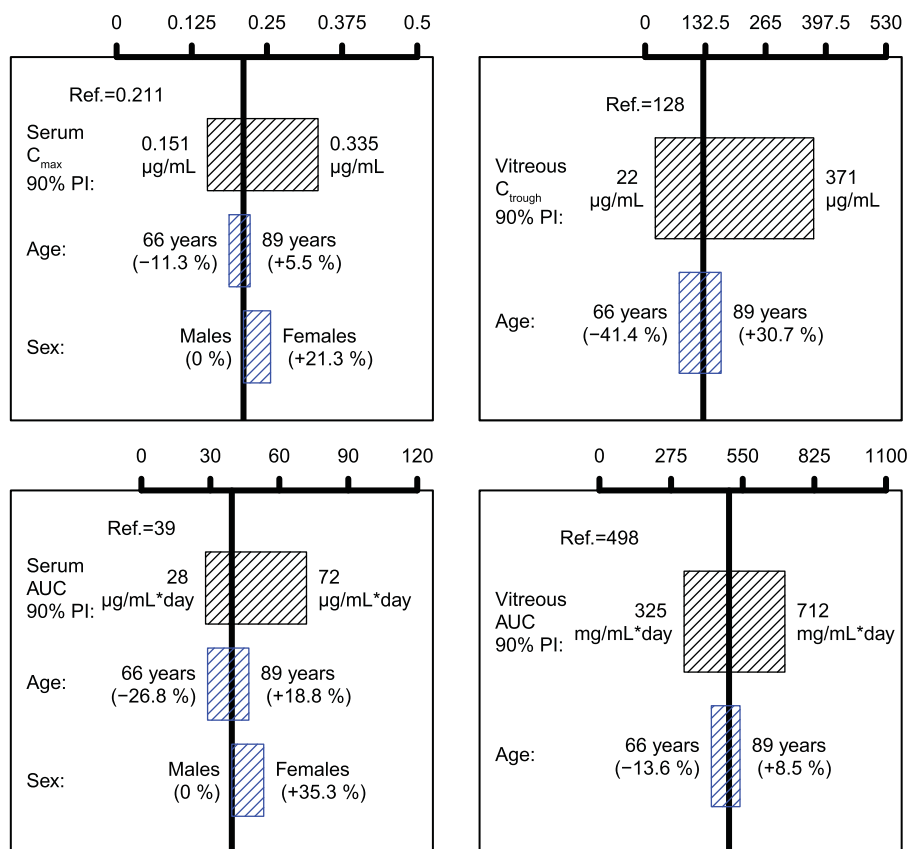


Figure 5 Impact of age and sex on serum and vitreous humor exposures. The black boxes illustrate the 90% prediction interval of individual exposures in the analysis population. The blue boxes correspond to the predictions of exposure for typical patients (80-year-old males) with the covariate values equal to 5th and 95th percentiles of the covariate distribution in the analysis population. AUC, area under the serum concentration time curve; C_{max} , maximum concentration; C_{trough} , minimum concentration; PI, prediction interval.

rate of 1.33 mg/kg/day (with a typical body weight of 75 kg).²⁷ These results were consistent with literature data on limited local ocular CFD production. Real-time quantitative polymerase chain reaction (PCR) analysis of complement CFD gene expression suggested limited production of CFD in the RPE-choroid and neural retina.²⁸

Our analysis also highlights the wide therapeutic index of ITV lampalizumab. Steady-state systemic exposures from ITV lampalizumab were substantially lower (11,000-fold) than ocular exposures. When administered monthly at a dose level of 10 mg per eye, vitreous humor trough concentrations were well above the IC₅₀ of alternative complement pathway inhibition within the eye while remaining substantially below the serum C_{min} required to inhibit systemic alternative complement activity. The low systemic exposure with ITV administration and the fast CFD production rate in the systemic circulation provided a potential mechanistic explanation for the suitable tolerability of lampalizumab ITV administration, which was shown in the phase I study.¹⁰ Increase of total CFD following dosing (Figure 3c) provided evidence of binding of lampalizumab to CFD in the eye. This was most likely due to slower clearance of drug-target complex

compared to clearance of free target and continuous ocular influx of systemic CFD. Increased levels of circulating ligand-drug complexes following administration of drug have been observed in other studies in the literature.^{11,29}

We evaluated the target occupancy in ocular tissues and systemic circulation using simulation studies to guide the dosing selection for the phase III studies (Chroma (NCT02247479) and Spectri (NCT02247531)). Our simulations predicted that the two dosing regimens (10 mg q4wk and 10 mg q6wk) selected for the phase III studies are expected to be efficacious and able to achieve near-complete target suppression in the vitreous humor (Figure 6). Additionally, these two regimens are expected to result in systemic drug concentrations substantially lower than the minimum level to elicit systemic CFD inhibition (Figure 4b) and provide strong scientific rationale for the recommended phase III dosing regimens.

Our analysis also revealed that both age and sex were statistically significant covariates for the systemic elimination rate constant (k). Older patients and females had a longer systemic half-life. It is likely that the impact of age and sex on systemic half-life may have been confounded by the underlying patient differences in renal clearance and body

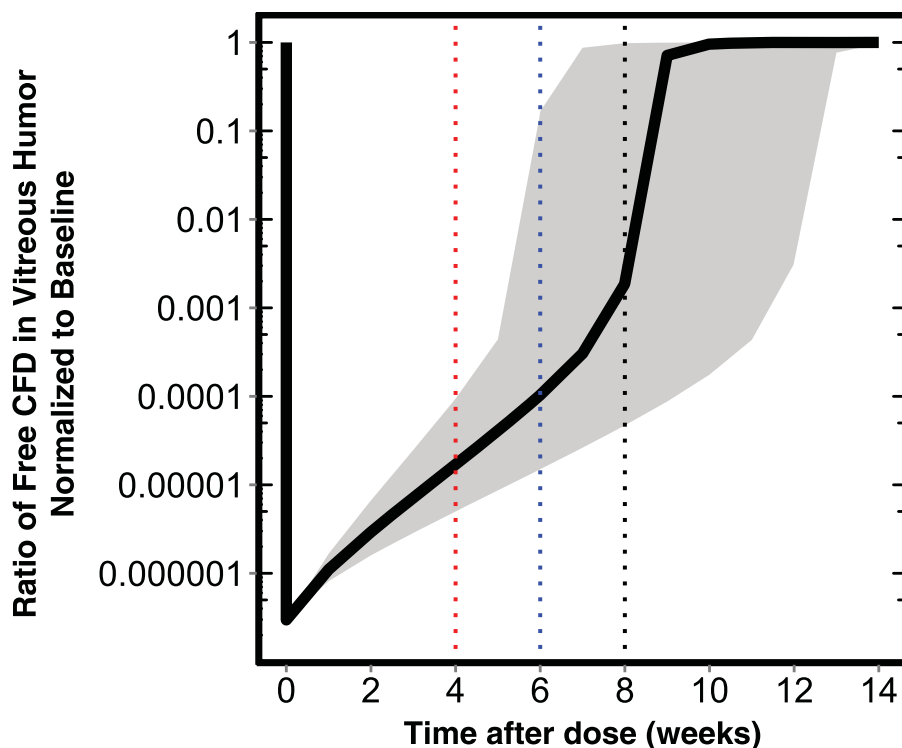


Figure 6 Simulations of free target suppression in vitreous humor expressed as ratio of free target to baseline over time. Solid black line represents the model-predicted vitreous humor free target ratio (FTR) for a typical patient in the CFD4870g study. Shaded region represents the 5th–95th prediction interval. Red, blue, and black lines denote the minimum FTR at 4, 6, and 8 weeks following intravitreal (ITV) lamalizumab administration. Black lines denote trend for a typical patient in CFD4870g study and shaded regions represent 5th–95th prediction intervals.

weight; however, these data were not available for these studies. The direction of the impact on systemic half-life was as expected based on the typical tendency of lower renal clearance in patients of older age, and lower body weight in females compared with males. The rapid systemic clearance of lamalizumab and the covariates of age and sex were in agreement with the existing literature, in which catalytic metabolism and renal clearance have been suggested to be mechanisms for systemic clearance of antibody binding fragments.^{19,30–32} The correlation between lamalizumab ocular half-life and age was an interesting finding. Older patients were shown to have a longer ocular half-life. Although there are limited data quantifying the effect of aging on ocular clearance of drugs, it has been shown that the vitreous body undergoes structural changes with aging.^{33,34} Despite the statistical significance, the covariate effect of age and sex on systemic half-life and age on ocular half-life of lamalizumab were not considered to be clinically relevant.

In conclusion, a semimechanistic modeling and simulation approach was implemented to analyze the phase I/II lamalizumab PK/PD data to provide an understanding of the ocular and systemic PK and PD of lamalizumab in patients with GA. These analyses represented the first TMDD model to guide rational study design in ophthalmology drug development. These results supported the dosing regimen selection for the phase III studies. The quantitative

framework presented here may help guide rational design of future clinical studies using lamalizumab.

Acknowledgments. Support for third-party writing assistance for this article was provided by Emma A. Platt, PharmD, at Envision Scientific Solutions and funded by Genentech, Inc. The authors thank William Hanley, PhD, for review and scientific input, and Shweta Vadavkar, MS, for clinical data assembly.

Author Contributions. K.N.L., L.G., M.L.C., J.G., T.D., A.M., E.C.S., and J.Y.J. wrote the article; K.N.L., J.G., T.D., A.M., and E.C.S. designed the research; K.N.L. and L.G. performed the research; K.N.L., L.G., J.G., T.D., A.M., and J.Y.J. analyzed the data.

Conflict of Interest/Disclosure. K.N.L. was an employee of Genentech, Inc. and is currently an employee of Agios Pharmaceuticals, Inc. K.N.L., M.L.C., J.G., T.D., K.M.L., A.M., E.C.S., and J.Y.J. are employees of Genentech, Inc. L.G. was a paid consultant for Genentech, Inc.

1. Wong, W.L. *et al.* Global prevalence of age-related macular degeneration and disease burden projection for 2020 and 2040: a systematic review and meta-analysis. *Lancet Glob. Health.* **2**, e106–116 (2014).
2. Sunness, J.S. *et al.* Visual function abnormalities and prognosis in eyes with age-related geographic atrophy of the macula and good visual acuity. *Ophthalmology.* **104**, 1677–1691 (1997).
3. Augood, C.A. *et al.* Prevalence of age-related maculopathy in older Europeans: the European Eye Study (EUREYE). *Arch. Ophthalmol.* **124**, 529–535 (2006).

4. Friedman, D.S. *et al.* Prevalence of age-related macular degeneration in the United States. *Arch. Ophthalmol.* **122**, 564–572 (2004).
5. Rees, A., Zekite, A., Bunce, C. & Patel, P.J. How many people in England and Wales are registered partially sighted or blind because of age-related macular degeneration? *Eye (Lond)*. **28**, 832–837 (2014).
6. Rees A. *et al.* Definition of blindness given in: United Kingdom Department of Health. Certificate of vision impairment explanatory notes for consultant ophthalmologists and hospital eye clinic staff. <https://www.gov.uk/government/uploads/system/uploads/attachment_data/file/213286/CVI-Explanatory-notes-in-DH-template.pdf>. Published 2013. Accessed November 10, 2014.
7. Lindblad, A.S. *et al.* Change in area of geographic atrophy in the Age-Related Eye Disease Study: AREDS report number 26. *Arch. Ophthalmol.* **127**, 1168–1174 (2009).
8. Katschke, K.J., Jr. *et al.* Inhibiting alternative pathway complement activation by targeting the factor D exosite. *J. Biol. Chem.* **287**, 12886–12892 (2012).
9. Tanhehco, E.J. *et al.* The anti-factor D antibody, MAb 166-32, inhibits the alternative pathway of the human complement system. *Transplant. Proc.* **31**, 2168–2171 (1999).
10. Do, D.V. *et al.* A phase Ia dose-escalation study of the anti-factor D monoclonal antibody fragment FCFD4514S in patients with geographic atrophy. *Retina.* **34**, 313–320 (2014).
11. Loyet, K.M. *et al.* Complement inhibition in cynomolgus monkeys by anti-factor D antigen-binding fragment for the treatment of an advanced form of dry age-related macular degeneration. *J. Pharmacol. Exp. Ther.* **351**, 527–537 (2014).
12. Avery, R.L. *et al.* Systemic pharmacokinetics following intravitreal injections of ranibizumab, bevacizumab or aflibercept in patients with neovascular AMD. *Br. J. Ophthalmol.* **98**, 1636–1641 (2014).
13. Bakri, S.J., Snyder, M.R., Reid, J.M., Pulido, J.S., Ezzat, M.K. & Singh, R.J. Pharmacokinetics of intravitreal ranibizumab (Lucentis). *Ophthalmology* **114**, 2179–2182 (2007).
14. Bakri, S.J., Snyder, M.R., Reid, J.M., Pulido, J.S. & Singh, R.J. Pharmacokinetics of intravitreal bevacizumab (Avastin). *Ophthalmology* **114**, 855–859 (2007).
15. Gaudreault, J. *et al.* Pharmacokinetics and retinal distribution of ranibizumab, a humanized antibody fragment directed against VEGF-A, following intravitreal administration in rabbits. *Retina.* **27**, 1260–1266 (2007).
16. Gaudreault, J., Fei, D., Rusit, J., Suboc, P. & Shiu, V. Preclinical pharmacokinetics of Ranibizumab (rhuFabV2) after a single intravitreal administration. *Invest. Ophthalmol. Vis. Sci.* **46**, 726–733 (2005).
17. Krohne, T.U., Eter, N., Holz, F.G. & Meyer, C.H. Intraocular pharmacokinetics of bevacizumab after a single intravitreal injection in humans. *Am. J. Ophthalmol.* **146**, 508–512 (2008).
18. Krohne, T.U., Liu, Z., Holz, F.G. & Meyer, C.H. Intraocular pharmacokinetics of ranibizumab following a single intravitreal injection in humans. *Am. J. Ophthalmol.* **154**, 682–686 e682 (2012).
19. Xu, L. *et al.* Pharmacokinetics of ranibizumab in patients with neovascular age-related macular degeneration: a population approach. *Invest. Ophthalmol. Vis. Sci.* **54**, 1616–1624 (2013).
20. Beal, S.L., Sheiner, L.B., Boeckmann, A.J. & Bauer, R.J. *NONMEM Users Guides. 1989-2013* (Icon Development Solutions, Ellicott City, MD, 2013).
21. Gibiansky, L., Gibiansky, E. & Bauer, R. Comparison of Nonmem 7.2 estimation methods and parallel processing efficiency on a target-mediated drug disposition model. *J. Pharmacokinet. Pharmacodyn.* **39**, 17–35 (2012).
22. Gibiansky, L., Gibiansky, E., Kakkar, T. & Ma, P. Approximations of the target-mediated drug disposition model and identifiability of model parameters. *J. Pharmacokinet. Pharmacodyn.* **35**, 573–591 (2008).
23. Xu, Z.H. *et al.* Population pharmacokinetics of golimumab in patients with ankylosing spondylitis: impact of body weight and immunogenicity. *Int. J. Clin. Pharmacol. Ther.* **48**, 596–607 (2010).
24. Ng, C.M., Stefanich, E., Anand, B.S., Fielder, P.J. & Vaickus, L. Pharmacokinetics/pharmacodynamics of nondepleting anti-CD4 monoclonal antibody (TRX1) in healthy human volunteers. *Pharm. Res.* **23**, 95–103 (2006).
25. Ng, C.M., Joshi, A., Dedrick, R.L., Garovoy, M.R. & Bauer, R.J. Pharmacokinetic-pharmacodynamic-efficacy analysis of efalizumab in patients with moderate to severe psoriasis. *Pharm. Res.* **22**, 1088–1100 (2005).
26. Avery, R.L., Le, K., Lu, T., Sternberg, G., Visich, J. Visual acuity response as a function of the affinity and vitreous half-life of intravitreally-administered anti-VEGF agents. Presented at the ASRS 30th Annual Meeting: August 28, 2012, Aria Resort, Las Vegas, NV.
27. Pascual, M., Steiger, G., Estreicher, J., Macon, K., Volanakis, J.E. & Schifferli, J.A. Metabolism of complement factor D in renal failure. *Kidney Int.* **34**, 529–536 (1988).
28. Anderson, D.H. *et al.* The pivotal role of the complement system in aging and age-related macular degeneration: hypothesis re-visited. *Prog. Retin. Eye Res.* **29**, 95–112 (2010).
29. Hayashi, N., Tsukamoto, Y., Sallas, W.M. & Lowe, P.J. A mechanism-based binding model for the population pharmacokinetics and pharmacodynamics of omalizumab. *Br. J. Clin. Pharmacol.* **63**, 548–561 (2007).
30. Lobo, E.D., Hansen, R.J. & Balthasar, J.P. Antibody pharmacokinetics and pharmacodynamics. *J. Pharm. Sci.* **93**, 2645–2668 (2004).
31. Renard, C., Grene-Lerouge, N., Beau, N., Baud, F. & Scherrmann, J.M. Pharmacokinetics of digoxin-specific Fab: effects of decreased renal function and age. *Br. J. Clin. Pharmacol.* **44**, 135–138 (1997).
32. Wochner, R.D., Strober, W. & Waldmann, T.A. The role of the kidney in the catabolism of Bence Jones proteins and immunoglobulin fragments. *J. Exp. Med.* **126**, 207–221 (1967).
33. Wang, J., McLeod, D., Henson, D.B. & Bishop, P.N. Age-dependent changes in the basal retinovitreal adhesion. *Invest. Ophthalmol. Vis. Sci.* **44**, 1793–1800 (2003).
34. Los, L.I., van der Worp, R.J., van Luyn, M.J. & Hooymans, J.M. Age-related liquefaction of the human vitreous body: LM and TEM evaluation of the role of proteoglycans and collagen. *Invest. Ophthalmol. Vis. Sci.* **44**, 2828–2833 (2003).

© 2015 The Authors CPT: Pharmacometrics & Systems Pharmacology published by Wiley Periodicals, Inc. on behalf of American Society for Clinical Pharmacology and Therapeutics. This is an open access article under the terms of the Creative Commons Attribution-NonCommercial-NoDerivs License, which permits use and distribution in any medium, provided the original work is properly cited, the use is non-commercial and no modifications or adaptations are made.

Supplementary information accompanies this paper on the CPT: Pharmacometrics & Systems Pharmacology website (<http://www.wileyonlinelibrary.com/psp4>)